Electron-impact ionization of In^+ and Xe^+

E. W. Bell, N. Djurić,* and G. H. Dunn†
Joint Institute for Laboratory Astrophysics, University of Colorado and National Institute of Standards and Technology, Boulder, Colorado 80309-0440
(Received 14 June 1993)

Absolute ionization cross sections for In^+ and Xe^+ by electron impact have been measured from below threshold to 200 eV using the crossed-beams technique. The cross sections for In^+ were possibly enhanced by indirect ionization processes. The excitation of the ion from the $4d^{10}5s^2$ ground state to the $4d^95s^25p$ state followed by autoionization has been postulated. The In^+ cross sections show a peak value of 15.9×10^{-17} cm^2 at about 80 eV. The cross sections for Xe^+ peak at a value of 25.6×10^{-17} cm^2 at about 35 eV. Experimental measurements are compared to configuration-averaged distorted-wave calculations [M. S. Pindzola *et al.*, J. Phys. B **16**, L355 (1983)], the semiempirical formula of Lotz [Z. Phys. **216**, 241 (1968)], and, in the case of Xe^+, previous experimental results [C. Achenbach *et al.*, J. Phys. B **17**, 1405 (1984)]. Also presented are ionization-rate coefficients and fitting parameters for both ions for temperatures in the range 10^4 K $\le T \le 10^7$ K.

PACS number(s): 34.80.Kw

INTRODUCTION

Absolute cross sections for electron-impact ionization of positive ions are important to many fields of research ranging from controlled nuclear fusion to astrophysics, and much effort has been expended studying ionization both experimentally [1] and theoretically [2]. However, due to the number of possible ionization mechanisms and the number of ions to study, much work remains to be done. Heavy ions in particular have received relatively little attention. In many cases, indirect processes, such as excitation-autoionization (EA), i.e., the excitation of an inner-shell electron followed by the expulsion of one or more electrons, can significantly enhance the total measured ionization cross section.

In the absence of experimental information, a number of quantum-mechanical and semiempirical formulas have been relied on for the necessary data. Difficulties with theoretical calculations for ionization lie in the number of ionization mechanisms available in addition to the many-body nature of the ionization process. For heavy ions possessing many electrons in outer electron shells, the modeling is even more complicated.

In^+ was chosen for study because it showed promise in promoting an understanding of heavy-ion ionization. It is in the same column of the Periodic Table as Ga^+, an ion that showed significant contributions to the ionization cross sections from indirect processes [3,4]. Reported in this paper are experimental results for absolute cross sections for electron-impact ionization of In^+, as well as an investigation of possible indirect contributions to cross sections near threshold. Also presented are measured cross sections for Xe^+, a heavy ion for which measurements have been previously performed. The relatively close proximity of Xe^+ to In^+ in the Periodic Table and the existence of previous measurements on Xe^+ made it a good benchmark case to demonstrate the correct functioning of the apparatus for these heavy ions.

EXPERIMENTAL METHOD

The experiments were performed using the crossed-beams method. This method has the advantage that all the quantities that determine the cross section can be measured independently, and thus absolute cross sections can be obtained. For beams at 90° the absolute single-ionization cross section σ at energy E is determined from the experimentally measured quantities by [1,5]

$$\sigma(E)=\frac{Re^2}{I_eI_i}\frac{v_iv_e}{(v_i^2+v_e^2)^{1/2}}\frac{F}{\epsilon}, \tag{1}$$

where R is the signal count rate, e is the electron charge, I_i, I_e, v_i, and v_e are the ion and electron currents and velocities, respectively, ϵ is the detector efficiency, and F is the form factor, a geometric quantity that takes the spatial overlaps of the two beams into account. The crossed-beams apparatus used for these experiments was similar to that used for several previous reports from this laboratory [3,6,7], so only a brief description is given here.

Ions were produced by a commercial hot-cathode discharge source [8], extracted and accelerated to 1200 eV. In^+ ions were produced by inserting a sample probe loaded with indium metal into the ion source where the heat from the source filament vaporized enough indium to maintain a discharge. Xe^+ ions were produced by introducing xenon gas into the source.

After collimation and mass selection, the ion beam was directed into the interaction region where it was crossed at 90° by a magnetically confined electron beam. Passing

*Permanent address: Institute of Physics, P.O. Box 57, 11001, Beograd, Yugoslavia.
†Quantum Physics Division, National Institute of Standards and Technology, Boulder, CO.

through the interaction region, the signal ions were separated from the parent ion beam by use of a 45° electrostatic analyzer. The signal ions were counted by an electron multiplier [9], and the parent beam was collected in a suppressed Faraday cup.

The electron gun is similar to that described by Taylor and Dunn [10,11]. An oxide coated nickel cathode produced electrons that were then formed into an electron beam immersed in a 200-G axial magnetic field. After interacting with the ion beam, the electrons were collected in a specially designed Faraday cup that was biased at 300 V to prevent the escape of secondary electrons and minimize reflection loss of electrons in the magnetic field. The energy spread of the beam was estimated at 0.3 eV full width at half maximum for the energy range of this experiment. The electron beam was chopped and scalers were synchronously gated at about 100 Hz to enable doubly charged ions that were created by interaction with the electron beam to be separated from ions created by collisions with background gas.

Form factors were determined by means of a movable thin-slit probe located in the interaction region. The probe was scanned vertically through each beam in turn, and currents were measured throughout the vertical extent of each beam.

The data for these experiments were taken in one of two modes. In the first mode, data were accumulated at a single electron energy until adequate statistical precision was obtained. The second mode of operation entailed scanning the electron energy repeatedly over several energies, accumulating data for 1 s at each energy, and storing the relevant parameters before moving on to the next energy. Accumulation continued until the desired statistical precision had been achieved. Typically, this took approximately 100–150 scans through the entire energy range. The advantage of taking data in this manner was that long-term drifts in the experimental parameters could be "averaged out," and relatively small structures in the cross section curve could then be seen. The points measured using this technique are not absolute because form factors were not taken at all the energies in the energy range, but they can be made absolute by normalizing to points measured using the first method that lie in the energy range being scanned.

To make the cross-section measurements absolute, the detection efficiency ϵ for each signal ion must be known. These values were determined in a separate experiment. In the present work some cross sections were measured with the detector wired as a Faraday cup connected to a high-sensitivity electrometer [12]. Signal currents and primary beam currents were recorded for extended periods of time, alternating times with the electrons "on" and "off" to separate the signal ions from the background ions. Absolute cross sections were determined by replacing R in Eq. (1) with $I_{2+}/2e$, where I_{2+} was the electrical current of the signal ions (typically less than 10^{-14} A) and by replacing ϵ with unity. The measurements made with the detector in a pulse counting mode were then normalized to this absolute measurement, and the detector efficiency for doubly charged ions was thus determined. Detection efficiencies ϵ determined using this method yielded 0.64 ± 0.08 for In^{2+} and 0.61 ± 0.04 for Xe^{2+}.

The ion-source discharge can populate metastable levels of both In^+ and Xe^+. Thus, to determine cross sections for ionization from the ground state, the raw data were corrected for signal counts due to metastable content of the parent ion beam. By observing signal below the ionization threshold, an estimate of the percentage of metastables in the ion beam could be deduced [13]. In the In^+ data presented here, the below-threshold points were fit with the Lotz-formula [14] prediction for ionization from the $4d^{10}5s5p$ metastable configuration. In the case of Xe^+, the Lotz-formula prediction for the $4d^{10}5s5p^6$ metastable configuration was used. Using this method, metastable fractions of 6% and 1% were deduced (leading to corrections at the peak of the cross-section curve of 1% and 3%) for In^+ and Xe^+, respectively.

The energy scale was calibrated by taking data using the scan mode over an energy range that included the threshold for ionization. After the data were corrected for metastable content of the ion beam, a straight line was fitted through the data near threshold. The contact potential, the difference between the cathode voltage and the true electron energy, was then shifted until the observed axis intercept of the fitted line corresponded to the spectroscopic value [15] for the ionization potential. The cathode was operated under a number of different conditions, and the shifts found ranged between 0.9 and 2.2 V, quite typical for values we have previously found with this type of cathode.

Special care was taken to ensure the collection and proper counting of all the signal ions. One complication of using a magnetically confined electron gun was that the magnetic field deflects the ion beam as it passes through the interaction region. Signal ions were deflected twice as much because they are doubly charged. Vertical ion deflectors located before and after the interaction region mitigate this problem, but careful beam tuning is required to guarantee that all the signal ions reached the detector. The preamplifier, amplifier, and electronics chain were also frequently checked throughout the experiments to verify that no spurious effects were corrupting the data.

RESULTS AND DISCUSSION

Experimental cross sections for electron-impact ionization of In^+ are shown in Fig. 1 and listed in Table I. The data have been corrected for metastable content of the parent ion beam. Absolute measurements are indicated by solid circles with error bars representing an expanded uncertainty [16] U_r defining a confidence level (CL) of about 90% (a coverage factor $k=2.0$ was used) for relative uncertainties. Relative uncertainties are those that may affect the shape of the curve as well as the value, and they are determined by a quadrature sum of contributions from uncertainties resulting from counting statistics, relative uncertainties in form factors, uncertainties in corrections for the metastable content of the ion beam, and fluctuations in the detector efficiency. The bold error

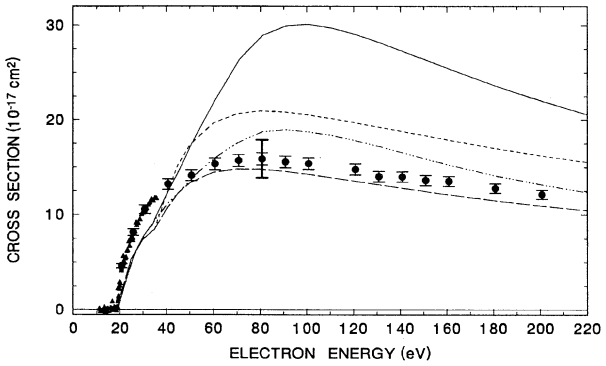

FIG. 1. Absolute cross section vs electron energy for the electron-impact single ionization of In^+: ●, present absolute measurements; ▲, data taken by scanning electron energies over a selected range and normalizing to absolute points within the energy range; ——, CADW calculations (Ref. [17]); - - -, Lotz formula; —·—·—·, modified CADW ($\frac{1}{2}d$ shell) calculations; — — —, modified ($\frac{1}{2}d$ shell) Lotz formula. Error bars represent U_r (see text) defining a CL of about 90% for relative errors, and the peak-value total absolute uncertainty (relative and systematic) is shown by the bold error bar at 80.8 eV.

bar in the figure at 80.8 eV represents total expanded uncertainty U_t including an additional ±12%, due to systematic uncertainties, added in quadrature with U_r. Systematic uncertainties affect the value of all points in the same manner. Contributions to the systematic uncertainties include those from signal ion collection, primary beam current collection, absolute uncertainties in the form factor, and absolute uncertainties in the detection efficiency.

TABLE I. Experimental cross sections for electron-impact single ionization of In^+. Expanded relative uncertainties U_r are listed, where a coverage factor $k=2.0$ has been used to set an approximate confidence interval on U_r of 90%. Total systematic uncertainties are estimated to be ±12%, with a similar confidence interval.

Energy (eV)	$\sigma\pm\Delta\sigma$ (10^{-17} cm^2)
20.8	4.6±0.2
25.8	8.1±0.4
30.8	10.5±0.5
40.8	13.2±0.6
50.8	14.1±0.6
60.8	15.3±0.6
70.8	15.7±0.6
80.8	15.9±0.6
90.8	15.6±0.6
100.8	15.4±0.6
120.8	14.8±0.6
130.8	14.0±0.6
140.8	14.0±0.6
150.8	13.6±0.5
160.8	13.5±0.5
180.8	12.8±0.5
200.8	12.1±0.5

All points are a weighted average of several data runs. Solid triangles represent the data taken in the "scan" mode discussed earlier. The solid curve in the figure represents the configuration-averaged distorted-wave (CADW) predictions of Pindzola [17]. Because of their wide use in cases where data from experiment or theory are not available, results using the semiempirical Lotz formula [14] (short dashed curve) are also presented. In this case, the single-parameter formula is used, even though it was presented by Lotz for use only for multiply charged ions. No parameters were presented by Lotz for In^+, and the results using the parameters for neutral In bear no resemblance to the data. Contributions from the 5*s* and 4*d* subshells were included in both the CADW and Lotz calculations.

There is clearly a large discrepancy between the observed and calculated values. Because of this, alternative calculations were made in which the contribution to the ionization cross section from electrons in the 4*d* subshell was added in at only one-half its calculated value. The results are the modified curves for the CADW and Lotz curves shown in Fig. 1 by the chain and the long dashed curves, respectively. Use of only half of the *d* subshell contributions was first proposed by Rogers *et al.* [3] and has since been shown to fit the experimental data better for several other experiments on singly [6] and multiply [18] charged ions. The present work supports this empirically based practice.

In a series of papers on giant resonances in electron-impact ionization, Younger [19] treated the *d* shell particularly carefully and used some arguments that help justify this arcane treatment of the *d* shell. In the CADW method, the *d*-shell contribution to the cross section is dominated by the 4*d*-*kf* ejection channel. The dominance of this channel is caused by ignoring term dependence in the $4d^9kf\ ^1P$ channel. The 4*d*-*kf* exchange interaction produces a double-well potential for the continuum electron with a potential barrier near the *d* shell. For lower impact energies, the *kf* partial wave will not be able to penetrate the barrier and overlap with the *d* shell, so a lower cross section is predicted. Younger's results taking this term dependence into account yield results that are virtually identical to the curve using the full *d* shell in the Lotz-formula predictions shown in Fig. 1.

The measured cross sections in Fig. 1 reach a peak value of $(15.9\pm0.6)\times10^{-17}$ cm^2 at approximately 80 eV after which they slowly decrease to the end of the energy range. The data rise faster than any of the theoretical curves up to about 40 eV. Above this energy the agreement between the experiment and the modified calculated curves is fairly good. Figure 2 shows the results for In^+ (solid triangles) in the region above threshold. Also shown are the CADW results of Pindzola (solid curve) and the semiempirical formula of Lotz (dashed curve). Since the maximum energy in Fig. 2 is lower than the ionization potential for *d*-shell electrons, only contributions from the *s* shell are taken into account for these curves. As already noted, the experimental points lie above the theoretical predictions for energies about 1 eV above threshold up to about 40 eV, probably indicating

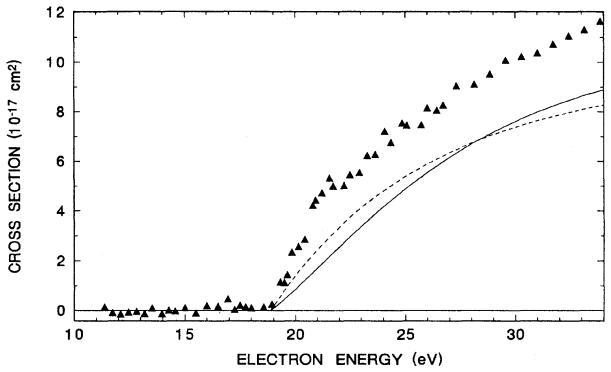

FIG. 2. Cross section for ionization of In^+ in the near-threshold region: ▲, data taken by scanning electron energies over a selected range; ——, CADW calculations, - - -, Lotz formula.

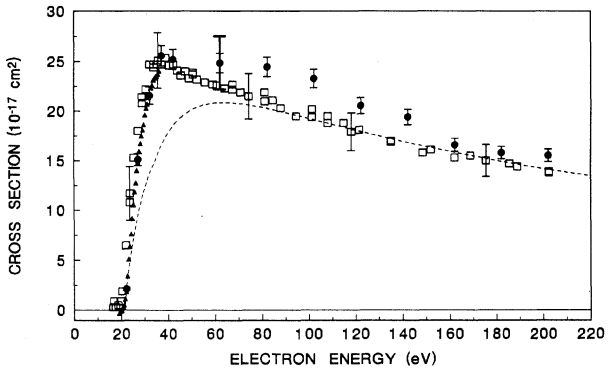

FIG. 3. Absolute cross section vs electron energy for the electron-impact single ionization of Xe^+: ●, present absolute measurements; ▲, data taken by scanning electron energies over a selected range and normalizing to absolute points within the energy range; □, experimental data of Achenbach *et al.* [22]; - - -, Lotz formula. Error bars for present data represent U_r (see text) defining a CL of about 90% for relative errors, and the peak-value total absolute uncertainty is shown by the bold error bar at 62.1 eV. Error bars for Ref. [22] represent total absolute uncertainty (see text).

contributions from EA in this region.

There is a sharp change in the slope of the cross-section curve at about 21 eV. Such changes in slope can often be attributed to indirect ionization processes, such as EA. One may postulate an excitation from the ground state $4d^{10}5s^2$ to the $4d^9 5s^2 5p$ excited state followed by autoionization to explain the change of the slope in Fig. 2. Using a simple quantum-defect approximation [20] to determine the excitation energy yields approximately the observed energy of the change in the slope. In any case, the contribution of indirect ionization processes to the total ionization cross section is small. Enhancements in the cross sections due to EA from the $3d$ subshell have been previously observed in Ga^+ [3].

Indirect contributions to the ionization cross section of In^+ have been treated theoretically by Pindzola, Griffin, and Bottcher [21]. They only took into account enhancements due to excitation from the $4d$ to the $4f$ subshell followed by autoionization. A small contribution to the total cross section was predicted at about 29 eV. However, the predicted contributions are smaller than our experimental error bars, and, in fact, no statistically significant change in the cross section was seen in this energy.

Experimental results in Xe^+ are plotted in Fig. 3 as solid circles with error bars representing U_r, and results are also listed in Table II. The bold error bar at 62.1 eV represents ±10% total expanded uncertainty U_t as discussed above. Cross sections measured using the scan mode are shown as solid triangles. Also displayed are the previous experimental results of Achenbach *et al.* [22] (open squares). Only a few representative error bars of these authors are included on select points. The error bars represent total absolute uncertainties, which were considered by Achenbach *et al.* to be equivalent to 95% CL. The present measurements are in good agreement with the previous results. Predictions from the single-parameter Lotz formula are represented by the dashed curve, and since ionization of a d shell electron leads to autoionization and hence a net double ionization, only the $5p$ and $5s$ subshells were included in the formula. Cross sections reach a peak value of $(25.6\pm1.0)\times10^{-17}$ cm^2 at about 35 eV. The experimental cross sections rise faster than the semiempirical prediction and remain significantly above the predicted curve up to about 100 eV. The agreement at higher energies is good. No attempt was made to attribute the steeper rise in cross sections to any specific ionization process.

In evaluating the Lotz formula for both In^+ and Xe^+, spectroscopic energies for the outermost electron came from Ref. [15] and the other energies came from Ref. [23].

TABLE II. Experimental cross sections for electron-impact single ionization of Xe^+. Expanded relative uncertainties U_r are listed, where a coverage factor $k=2.0$ has been used to set an approximate confidence interval on U_r of 90%. Total systematic uncertainties are estimated to be ±10%, with a similar confidence interval.

Energy (eV)	$\sigma\pm\Delta\sigma$ (10^{-17} cm^2)
22.1	2.1±0.1
27.1	15.1±0.6
32.1	21.6±0.9
37.1	25.6±1.0
42.1	25.2±1.0
62.1	24.9±1.0
82.1	24.5±1.0
102.1	23.3±0.9
122.1	20.6±0.8
142.1	19.4±0.8
162.1	16.6±0.7
182.1	15.8±0.6
202.1	15.5±0.6

TABLE III. Rate coefficients $\alpha(T)$ (in cm^3/s) for the ionization of In^+ and Xe^+ at selected values of temperature (in K). Numbers in brackets are powers of 10.

T (K)	In^+	Xe^+
1.000[+4]	9.765[−18]	7.317[−19]
2.000[+4]	6.755[−13]	2.477[−13]
4.000[+4]	1.867[−10]	1.693[−10]
6.000[+4]	1.265[−9]	1.566[−9]
8.000[+4]	3.375[−9]	4.820[−9]
1.000[+5]	6.184[−9]	9.504[−9]
2.000[+5]	2.252[−8]	3.750[−8]
4.000[+5]	4.709[−8]	7.514[−8]
6.000[+5]	6.164[−8]	9.402[−8]
8.000[+5]	7.070[−8]	1.046[−7]
1.000[+6]	7.664[−8]	1.111[−7]
2.000[+6]	8.784[−8]	1.232[−7]
4.000[+6]	8.879[−8]	1.253[−7]
6.000[+6]	8.582[−8]	1.226[−7]
8.000[+6]	8.265[−8]	1.193[−7]
1.000[+7]	7.975[−8]	1.160[−7]

RATE COEFFICIENTS

It is often desirable to have ionization data in the form of rate coefficients rather than cross sections. Rate coefficients are calculated from ionization data by integrating the product of the ionization cross sections and electron velocity, which are assumed to have a Maxwellian distribution, following the procedure used by Crandall *et al.* [24].

Table III presents rate coefficients calculated at several temperatures using the reported data. The rate coefficients were fit with Chebyshev polynomials to allow the user to calculate rate coefficients $\alpha(T)$ at any temperature 10^4 K $\leq T \leq 10^7$ K by evaluating the expansion

$$\alpha(T)=e^{-I/kT}T^{1/2}\sum_{r=1}^{n} a_r T_r(x), \quad x=\frac{\log_{10}T-5.5}{1.5}, \tag{2}$$

where I is the ionization energy in eV, k is the Boltzmann constant, $T_r(x)$ are Chebyshev polynomials, and the a_r are expansion coefficients that fit the data. The a_r are listed in Table IV.

TABLE IV. Expansion coefficients for generating ionization rate coefficients for In^+ and Xe^+. Numbers in brackets are powers of 10.

Coefficient	In^+	Xe^+
a_0	2.998 49[−10]	4.510 13[−10]
a_1	−1.408 69[−10]	−1.926 73[−10]
a_2	1.822 50[−11]	−2.684 10[−11]
a_3	−4.861 63[−12]	4.132 29[−11]
a_4	1.962 81[−12]	−7.213 01[−12]
a_5	3.320 22[−12]	−5.026 21[−12]
a_6	−1.837 38[−12]	3.168 04[−12]
a_7	−8.679 08[−14]	−6.464 37[−13]

Using Clenshaw's algorithm [25], the $\alpha(T)$ can be expressed by

$$\alpha(T)=\tfrac{1}{2}T^{1/2}e^{-I/kT}(b_0-b_2), \tag{3}$$

where

$$b_{n+2}=b_{n+1}=0, \tag{4}$$

$$b_r=2xb_{r+1}-b_{r+2}+a_r, \quad r=n,n-1,\ldots,0. \tag{5}$$

CONCLUSIONS

Cross sections have been measured for both In^+ and Xe^+ from below threshold to 200 eV. Enhancements to the cross sections for In^+ have been tentatively attributed to excitation of a $4d$ electron followed by autoionization. The observed cross sections are in poor agreement with the CADW and Lotz-formula predictions. However, when only half the d subshell contribution is applied in calculations, the agreement is good at high energies. Cross sections for Xe^+ were in good agreement with previous measurements.

ACKNOWLEDGMENT

This work was supported in part by the Office of Fusion Energy of the U.S. Department of Energy under Contract No. DE-A105-86ER53237 with the National Institute of Standards and Technology.

[1] See G. H. Dunn, in *Electron Impact Ionization*, edited by T. D. Märk and G. H. Dunn (Springer-Verlag, New York, 1985), p. 277.
[2] See S. M. Younger, in *Electron Impact Ionization* (Ref. [1]), p. 1.
[3] W. T. Rogers, G. Stefani, G. Camilloni, G. H. Dunn, A. Z. Msezane, and R. J. W. Henry, Phys. Rev. A **25**, 737 (1982).
[4] B. Peart and J. R. A. Underwood, J. Phys. B **23**, 2343 (1990).
[5] K. T. Dolder and B. Peart, Rep. Prog. Phys. **39**, 693 (1976).
[6] D. S. Belić, R. A. Falk, C. Timmer, and G. H. Dunn, Phys. Rev. A **36**, 1073 (1987).
[7] N. Djurić, E. W. Bell, E. Daniel, and G. H. Dunn, Phys. Rev. A **46**, 270 (1992).
[8] M. Menzinger and L. Wahlin, Rev. Sci. Instrum. **40**, 102 (1969).
[9] Johnston Laboratories, Model No. MM-1 electron multiplier. Model number and manufacturer are given for technical completeness and are not meant as a product endorsement.
[10] P. O. Taylor and G. H. Dunn, Phys. Rev. A **8**, 2304 (1973).
[11] P. O. Taylor, K. T. Dolder, W. E. Kappila, and G. H. Dunn, Rev. Sci. Instrum. **45**, 538 (1974).
[12] Cary Model No. 31 and Keithley Model No. 642 electrometers were used. Model numbers and manufacturers are included for technical completeness only and are not

meant as a product endorsement.
[13] See procedure in N. Djurić, E. W. Bell, X. Q. Guo, G. H. Dunn, R. A. Phaneuf, M. E. Bannister, M. S. Pindzola, and D. C. Griffin, Phys. Rev. A **47**, 4786 (1993).
[14] W. Lotz, Z. Phys. **216**, 241 (1968).
[15] C. E. Moore, *Atomic Energy Levels,* Natl. Bur. Stand. (U.S.) Circ. No. 467 (U.S. GPO, Washington, DC, 1949).
[16] Uncertainties are presented as per the guidelines in B. N. Taylor and C. E. Kuyatt, NIST Technical Note 1297, 1993 (unpublished).
[17] M. S. Pindzola (private communication). See also M. S. Pindzola, D. C. Griffin, and C. Bottcher, J. Phys. B **16**, L355 (1983).
[18] D. C. Gregory, P. F. Ditner, and D. H. Crandall, Phys. Rev. A **27**, 724 (1983).
[19] S. M. Younger, Phys. Rev. A **35**, 4567 (1987).
[20] K. Bartschat (private communication).
[21] M. S. Pindzola, D. C. Griffin, and C. Bottcher, Phys. Rev. A **27**, 2331 (1983).
[22] C. Achenbach, A. Müller, E. Salzborn, and R. Becker, J. Phys. B **17**, 1405 (1984).
[23] E. Clementi and C. Roetti, At. Data Nucl. Data Tables **14**, 177 (1974).
[24] D. H. Crandall, G. H. Dunn, A. Gallagher, D. G. Hummer, C. V. Kunasz, D. Leep, and P. O. Taylor, Astrophys. J. **191**, 789 (1974).
[25] C. W. Clenshaw, Math. Tables Comput. **9**, 118 (1955).